Green Chemistry

PAPER

View Article Online
View Journal | View Issue

Cite this: *Green Chem.*, 2026, **28**, 7459

Evaluating the sustainability of electrochemical CO_2 capture technology through LCA and LCC: a winery industry application

Prince S. A. Nopuo, †[a] Javiera Francisca Gutiérrez-Espinoza,†[a] Carmen M. Fernández-Marchante,*[a] Pedro M. Izquierdo-Cañas,[b] Esteban García,[b] Manuel A. Rodrigo [a] and Justo Lobato *[a]

This study presents a comprehensive environmental and economic assessment of CO_2 absorption using electrochemically produced NaOH for industrial decarbonization (*e.g.*, the winery industry). The EDEN® technology, based on the chlor-alkali electrochemical process, achieved high CO_2 capture efficiencies of up to 80%, with comparable performance when tested on pure CO_2 and fermentation-derived CO_2 streams (deviations <2%). Beyond capture, the system demonstrated multifunctionality by converting low-concentration waste brine (0.05–0.15 M) into hydrogen and chlorine while simultaneously fixing CO_2 as sodium carbonate or bicarbonate. Under optimized operating conditions, faradaic efficiencies for hydrogen production reached 98–100%, with energy consumption values of 3.10 kWh kg^{-1} NaOH at 5.5 V and 4.36 kWh kg^{-1} NaOH at 6.5 V, highlighting the trade-off between kinetics and energy intensity. Life-cycle and techno-economic analyses modeled four EDEN® scenarios and benchmarked them against conventional column absorption using commercial NaOH. Net carbon savings were demonstrated, with scenario 2 (electroabsorption) recording the lowest impacts across all categories (*e.g.*, −0.882 g CO_2-eq. and 32 mL_{water} per g CO_2 captured). Both carbon saving and capture costs were found to be highly sensitive to electricity carbon intensity. However, integration with renewable energy and the commercialization of co-products (H_2, Cl_2, Na_2CO_3) enabled capture costs to approach net-zero or even become negative. These findings underscore the significant climate-mitigation potential of electrochemical CO_2 capture when integrated into industrial processes. By combining CO_2 absorption with the co-production of valuable chemicals and hydrogen, EDEN® offers a scalable and versatile pathway toward environmentally and economically viable decarbonization, with direct applicability to the wine sector and broader industrial systems facing biogenic or process-related emissions.

Received 16th January 2026,
Accepted 8th April 2026

DOI: 10.1039/d6gc00309e

rsc.li/greenchem

Green foundation

1. This work advances green chemistry by demonstrating an integrated electrochemical carbon capture system powered by renewable energy that converts CO_2 into stable mineral carbonates while producing valuable chemicals (H_2, Cl_2) as co-products. Through experimentation and life cycle assessment, this study operationalized and validated key green chemistry principles: renewable energy use, waste valorization, process integration, and circularity.

2. In terms of technical feasibility, the designed system achieved CO_2 capture efficiencies of ~80% from real wine fermentation emissions. A scenario-based life cycle assessment shows that scenario 2 (electro-absorption powered by solar energy) achieved a net negative carbon footprint of −0.882 g CO_2-eq. per g CO_2 captured, translating to ~11.4% reduction in the carbon footprint of a bottle of wine. The system achieved a water footprint of 32 mL per g CO_2 captured and a capture cost of –€0.22 per kg CO_2, demonstrating its resource efficiency and economic viability.

3. The energy consumption was identified as a key contributor to the system carbon footprint; as a result, further research should focus on lowering the specific energy consumption through optimized cell architecture and improved ion transport. Additionally, replacing critical and high-impact materials (*e.g.*, noble-metal catalysts) with low-toxicity alternatives would further minimize the system's life cycle impacts.

[a]*Chemical Engineering Department, Faculty of Chemical Sciences and Technology, University of Castilla-La Mancha, Avda. Camilo José Cela 12, 13071 Ciudad Real, Spain. E-mail: carmenm.fmarchante@uclm.es, justo.lobato@uclm.es*
[b]*Instituto de la Vid y el Vino de Castilla-La Mancha (IVICAM), Instituto Regional de Investigación y Desarrollo Agroalimentario y Forestal, Ctra. Toledo-Albacete s/n, 13700 Tomelloso (Ciudad Real), Spain*
† Equally contributing authors.

Introduction

Climate change, the major environmental challenge of the 21st century, is caused by a rise in the atmospheric concentration of Greenhouse Gases (GHGs), mainly methane (CH_4), carbon dioxide (CO_2), and nitrous oxide (N_2O).[1] These gases arise from anthropogenic activities, and their accumulation in

the atmosphere poses a severe danger to human lives, the quality of the environment, and the economy at large.[2] Among these gases, CO_2 accounts for the largest share, and its emissions are primarily from the combustion of fossil fuels for energy production and from other industrial processes. From annual near-zero CO_2 emission, anthropogenic activities now account for 37.8 Gt CO_2, 50% higher than pre-industrial levels, according to the IEA 2024 report.[3]

In this regard, the implementation of Carbon Capture, Utilization, and Storage (CCUS) technologies in industrial processes is recognized as a promising strategy for decarbonization.[4,5] CCUS technologies are classified into three main categories: pre-combustion, post-combustion, and oxy-fuel combustion capture. The post-combustion capture approach involves capturing CO_2 at the point of emission for subsequent storage or utilization. This process involves absorption with solvents, adsorption by solid sorbents, membrane separation, and cryogenic separation.[6] Within the solvent-based absorption, amine scrubbing is the benchmark process for post-combustion capture. An emerging alternative process to amine scrubbing is the use of electrochemically produced sodium hydroxide to fix CO_2 in the form of carbonate.[7,8] The reaction pathways are provided in the SI. These reaction mechanisms underpin the development of an Electrochemical-based Decarbonization Energy (EDEN®) technology by our research group at the University of Castilla-La Mancha.

The developed EDEN® technology, employs a unitized cell, based on the chlor-alkali electrochemical process, to operate in both electrolysis and fuel cell modes. By electrolyzing brine (NaCl solution), it produces valuable co-products like hydrogen (H_2) and chlorine (Cl_2), while the resulting sodium hydroxide (NaOH) captures CO_2 emissions by converting the gas into stable carbonates. Powered by renewable energy and suitable for any application with CO_2 emissions, EDEN® aims to reduce carbon footprints and promote energy self-sufficiency through an innovative integrated design. The theory of the electrolysis reactions can be found in the SI.

In the context of CO_2 capture, the EDEN technology can be integrated into any process where CO_2 emissions exist. Among the many sectors, the wine industry is a key player in the agriculture, forestry, and land use sector, a sector responsible for approximately one-fifth of the global GHG emissions.[9] The winery is a key component of the global agri-food sector and a major share of Europe's agricultural economy, especially in countries such as Spain, Italy, and France.[10] These are the top wine producers globally, collectively accounting for over 53% of the total wine production. As a production sector, activities across its supply chain, from grape cultivation through to distribution, contribute to global carbon emissions. For instance, Gazulla *et al.*[11] reported that the viticulture stage of Spanish wine production usually contributes about 15–30% of the total emissions in the winery. Agricultural activities such as soil tillage, pesticide use, irrigation, and the operation of machinery result in fossil fuel consumption with direct carbon emissions. The winemaking process is also a crucial phase. This phase involves fermentation, stabilization, cooling, and bottling, which accounts for about 17% of the overall CO_2 emissions.[12] The fermentation is a biological process, where yeast acts on sugars, breaking them down into ethanol, producing CO_2 as a byproduct, according to eqn (1).

$$C_6H_{12}O_6 \rightarrow 2C_2H_5OH + 2CO_2 \quad (1)$$

Although biogenic in nature, these emissions constitute a relevant share of the direct GHG emissions at the winery.

Although modest compared with other industrial processes, the global scale of wine production means that these emissions represent a significant mitigation opportunity. Recent research has shown that, although fermentation CO_2 accounts for only a small fraction of the total carbon footprint of wine, its magnitude is biogenically relevant. According to the vineyard–winery system evaluated by Pattara *et al.*[13] vineyards can sequester approximately 0.38 kg of CO_2 per litre of wine produced, whereas alcoholic fermentation returns a much smaller amount to the system. Stoichiometric calculations and published experimental data indicate that wine fermentation typically generates between 70 and 115 g of CO_2 per litre of wine,[12–14] which corresponds to approximately 10–11.5 kg of CO_2 per 100 L of wine with 13.5% v/v alcohol content.[13–15] These values highlight the role of vineyards as short-cycle carbon sinks, even though this uptake is not included in product carbon footprint calculations according to LCA standards (Neto *et al.*, 2013). Within the framework of LCA, all environmental burdens associated with the vineyard are attributed solely to the wine, since it is the only output flow with economic value for the grower. The economic viability of vineyard operations depends exclusively on the wine sold; therefore, other potential products obtained from grapes or grape residues (ethanol, antioxidant compounds, grape seed oil, among others) are not considered relevant co-products for allocation purposes.

The global annual wine production for 2024 was reported to be 225.8 million hectolitres,[15] which means the total emissions from fermentation alone can be estimated to be about 2.6 million tons of CO_2. While this amount may be smaller than other industrial processes, its capture is equally important, as every kilogram of CO_2 captured is a step toward net-zero emissions. Additionally, the capture of CO_2 emissions from the winery is key to reducing the industry's carbon footprint and ensuring its sustainability.

The possibility of capturing and stabilising part of this biogenic CO_2 before it returns to the atmosphere offers a promising pathway to enhance the climate mitigation potential of the wine sector. Electrochemical technologies such as EDEN®, based on chlor-alkali electrolysis, allow fermentation CO_2 to be converted into stable carbonate salts (Na_2CO_3/$NaHCO_3$). The work of Flor Montalvo *et al.*[14] demonstrated that electrochemically produced NaOH can be effectively used for CO_2 absorption, providing an opportunity for local and long-term carbon storage at a winery scale.

While this process presents great potential for combating climate change, its implementation involves downstream and upstream environmental trade-offs that could compromise its overall sustainability. This highlights the need for a detailed evaluation of the process environmental performance over its life cycle. In this regard, life cycle assessment (LCA) helps in identifying hidden environmental impact hotspots, such as energy use and water consumption, and resource depletion within the technology life cycle, even though it is intended to reduce emissions.[16]

In this work, we employed an integrated methodology to comprehensively assess the sustainability of integrating the EDEN® technology into the winery. We demonstrated the successful capture of CO_2 from wine fermentation emissions *via* two capture approaches: column absorption using electrochemically produced NaOH and electro-absorption (CO_2 absorbed directly in the electrochemical cell without an absorption column). The operation conditions of these two approaches were optimized to achieve high carbon capture efficiencies. Based on the optimal conditions and performance, a scenario-based comparative life cycle assessment and life cycle costing were conducted. The scenarios modelling considered the two capture approaches, two types of electrochemical cell designs, and the potential of using commercial NaOH as a solvent in column absorption. Altogether, 5 scenarios were evaluated in terms of carbon footprint, water footprint, and toxicity impacts, along with the analysis of the capture cost.

The novelty of this work, therefore, lies in the integration of electrochemical NaOH production with decentralized CO_2 capture in the context of the wine industry, combined with a comprehensive environmental and economic assessment. In contrast to previous studies that have mainly focused on laboratory-scale electrochemical carbon capture or conventional chlor-alkali systems, this work evaluates the coupling of EDEN-based brine electrolysis with both electro-absorption and conventional column absorption using real fermentation-derived CO_2 streams. The study further extends beyond process performance by including a combined life cycle assessment (LCA) and life cycle costing (LCC), sensitivity analysis to electricity supply, and break-even evaluation of electricity carbon intensity, allowing the environmental and economic viability of decentralized implementation to be assessed. This integrated approach provides new insight into the feasibility of using electrochemically generated alkalinity for on-site CO_2 utilization in production sectors generating biogenic or process-related CO_2 emissions.

Materials and methods

The work was carried out in two main stages. First, various operational conditions of two CO_2 capture approaches were experimentally optimized, with three different cell configurations for the electrolysis. The tested configurations included column absorption for CO_2 capture and electro-absorption of CO_2 using pure CO_2. Additionally, a case study was conducted on CO_2 capture from wine fermentation to simulate real-world CO_2 capture. Then, a life cycle assessment (LCA) and life cycle cost analysis (LCC) were performed based on the optimal experimental conditions. A schematic of the experimental methodology is shown in Fig. 1.

Step 1: laboratory-based optimization of the EDEN® process

Materials. The brine was prepared with NaCl, with 99.9% purity purchased from Sigma-Aldrich, USA, and deionized water sourced from a Milli-Q system. For the optimization process, pure CO_2 with a purity of ≥99.98% purchased from Air Liquide (ALPHAGAZ™, Spain) was used. For the fermentation, musto (grape juice) was purchased from a supermarket in Spain, and the yeast used was *Saccharomyces cerevisiae* strain, Uvaferm VN™ (Lallemand Oenology), selected by IVICAM (Wine and Vine Institute of Castilla-La Mancha, Spain). Nutrient Vit Nature, purchased from Lallemand Oenology in Canada, was used as a nutrient to accelerate wine fermentation.

Experimental setup for the electrolysis. Following the EDEN® technology design, a bench-scale chlor-alkali electrolysis setup was used. The electrolysis setup includes an electrochemical cell, 3D-printed tanks with gasometers, two G928 peristaltic pumps, silicon pipes, and a power inverter. Three electrochemical cell types (A, B, and C) were studied; their materials are presented in Table 1. The cell is a PEM system assembled from various 3D-printed components, designed with Fusion 360 (Autodesk) and printed with a 3D printing machine purchased from Formlabs Inc. (USA). All cells utilized a Nafion® N-117 PEM as the separator between the compartments. The cell consists of two compartments, with separate sections for the anode and cathode, and a central slot to accommodate the membrane electrode assembly (MEA). The

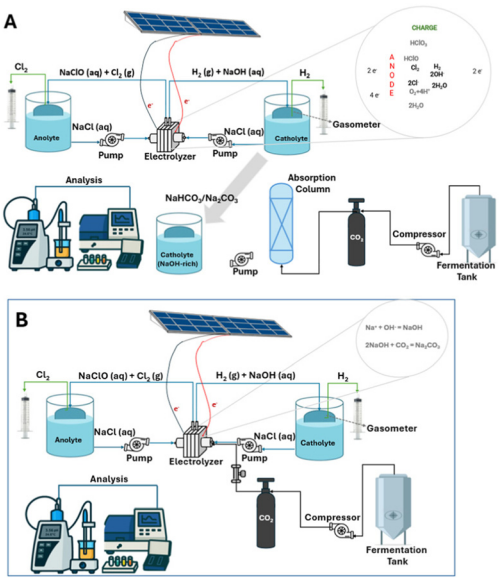

Fig. 1 General scheme of the methodology employed (A) column absorption, (B) electro-absorption.

Table 1 Summary of electrolyzer cell configurations

Cell type	Anode type	Electrode gap (cm)	Cathode type	Electrode size (cm^2)
Cell A	Commercial DSA® plate	3.0	Titanium plate (perforated with holes)	4 × 4
Cell B	Commercial DSA® plate	1.6	Titanium plate (perforated with holes)	4 × 4
Cell C	Lab made TiO_2/RuO_2-Pt anode	1.6	Titanium plate (perforated with holes)	4 × 4

MEA is in a "non-zero-gap" setup, where the anode, membrane, and cathode are separated by an electrode gap distance as shown in Table 1. The anodic compartment has a liquid stream inlet and outlet, while the cathodic compartment is designed to have a gas stream inlet, a liquid stream inlet, and one outlet. The same cathode was used in all three cell types: a 16 cm^2 titanium plate with 160 small holes (0.5 mm in diameter). The procedure for the synthesis of the lab-made TiO_2/RuO_2-Pt anodic electrode can be found in our previous work.[17] The electrochemical cells were designed to ensure a highly turbulent flow of the electrolytes and efficient gas release. The same cathode was used in all three cell types: a 16 cm^2 titanium plate with 160 small holes (0.5 mm in diameter). The electrochemical cells were designed to ensure a highly turbulent flow of the electrolytes and efficient gas release.

A 2 M NaCl solution (brine) was used as the electrolyte, based on a previous study.[17] In each experiment, the volume of anolyte and catholyte was set at 0.8 L each.

The electrolytes were fed into the system through the liquid stream inlets of both compartments in a recirculation mode, with the flow rates regulated by the pumps. The electrolysis was initiated with an applied voltage, producing H_2, Cl_2, and NaOH. Samples were taken from each compartment at 15-minute intervals to measure the pH, and the chlorine species concentration in both compartments was measured with a UV/Vis Spectroquant® PROVE 300 (Merck).

The pH of the catholyte was then used to calculate the NaOH concentration. The volume of the gas from each compartment was also measured to determine the gas production rate. The main variables studied for this process were the applied voltage, 5.5 V and 6.5 V, the electrolysis duration, and the cell type. The electrolysis types herein are labelled as A5.5, A6.5, B5.5, B6.6, C5.5, and C6.5, where the A, B, and C stand for the cell type, while 5.5 and 6.5 indicate the applied voltage.

CO_2 capture *via* column absorption approach. The CO_2 capture *via* column absorption is an integrated system of a chloro-alkali electrolysis and column absorption (Fig. 1A). Following the electrolysis process described in the preceding section, once the electrolysis was completed, the catholyte, which had now become NaOH-rich, was used as the solvent in a counter-flow column absorption to capture CO_2. The volume of the NaOH solvent was fixed at 0.8 L, and the variables studied were the CO_2 flow rate, NaOH flow rate, and NaOH concentration. The capture process conditions were initially optimized using pure CO_2, and then these conditions were applied to capture CO_2 from the wine fermentation. For the optimization of the studied variables, a central composite design of experiment was employed. The formation of Na_2CO_3 and $NaHCO_3$ was analyzed by titrating the solvent with a 0.05 M H_2SO_4, first from the initial pH to 8.3 to measure $NaHCO_3$, and then from 8.3 to 4.5 to measure Na_2CO_3. The concentration of the $Na_2CO_3/NaHCO_3$ was converted to moles and then used to determine the CO_2 capture efficiency.

CO_2 capture *via* the electro-absorption approach. The integrated system for electrochemical absorption of CO_2 was designed to produce NaOH, H_2, and Cl_2, while absorbing CO_2 simultaneously (Fig. 1B). The setup is a chlor-alkali electrolysis unit, as described in the electrolysis process, except that CO_2 was introduced into the system *via* the cathodic compartment gas inlet stream. The main variables studied for this process were the applied voltage, 5.5 and 6.5 V, the experiment duration, the CO_2 flow rate (8, 10, 15, 20, and 22 Nml min^{-1}), and the time for feeding CO_2 (at t = 0 min and t = 90 min). These factors were studied with the different electrolyzers. The capture experiments are identified as A1, A2, A3, B1, B2, B3, C1, C2, and C3, where the letters for the type of cell and the numeric indices 1, 2, and 3 denote a specific case of experimental conditions:

- Case 1. Applies 5.5 V, CO_2 feed at t = 0 min, and experiment duration of 60 min
- Case 2. Applies 6.5 V, CO_2 feed at t = 0 min, and experiment duration of 60 min
- Case 3. Applies 5.5 V, CO_2 feed at t = 90 min, and experiment duration of 150 min

As the electrolysis began, the produced NaOH instantly reacted with the CO_2 to form $Na_2CO_3/NaHCO_3$. The unreacted CO_2 left the cell and was collected at the gasometer as an H_2/CO_2 gas mixture. Samples were taken from each compartment at 15-minute intervals to measure the pH, and the $Na_2CO_3/NaHCO_3$ concentration in the catholyte was determined *via* titration with a 0.05 M H_2SO_4. The chlorine species concentration in both compartments was also measured with UV/Vis Spectroquant® PROVE 300 (Merck). The volume of the gas from each compartment was also measured at 15-minute intervals to determine the gas production rate. The H_2/CO_2 gas mixture was further passed through a 3 M NaOH solution to remove the unreacted CO_2, and the volume of H_2 at each time was used to calculate the hydrogen efficiency. The concentration of the $Na_2CO_3/NaHCO_3$ was converted to moles and then used to determine the CO_2 capture efficiency.

Wine fermentation to produce CO_2. The wine fermentation was done using must (grape juice), yeast, and yeast nutrients following a recipe provided by the Wine and Vine Institute of Castilla-La Mancha, Spain. After every 24 hours of fermentation, the gas from the fermentation tank was sucked and compressed with a mini diaphragm air compressor (Uniquers) into

a gas cylinder and then fed into the carbon capture system in a procedure similar to that used for pure CO_2. The same measurements and analysis described above were performed for each experiment. Additionally, the mass, temperature, and probable alcohol content of the fermentation broth were measured. The process was repeated daily until the fermentation was completed.

Main oenological parameters were analysed according to the official International Organisation of Vine and Wine (OIV) analytical methods (OIV, 2025). These included degree Brix, alcoholic content, total acidity, and pH. Concentrations of glycerol and tartaric, citric, lactic, succinic, and acetic acids were obtained by HPLC-IR, also according to the official OIV analytical methods. Glucose, fructose, and malic acid were analysed by an automated enzymatic method.

Step 2: Life cycle assessment (LCA) and life cycle cost (LCC) of the technology

Life cycle assessment. Once the experimental phase was conducted, the collected data were based on the most relevant configurations, determined by the compromise between NaOH production, CO_2 captured, and energy efficiency of each case. Based on the experimental results, cell A was not considered for the LCA and LCC studies because it performed poorly compared to cell B, in terms of evaluating the hydrogen, chlorine, and sodium hydroxide production, and energy utilization efficiency.

LCA was performed according to the methodological framework and guidelines from ISO 14040 and ISO 14044, using SimaPro 10.1.0.6. It involved selecting the relevant or most similar materials, making reasonable estimations, and utilizing the Ecoinvent 3.10 database.

For studying the Global Warming Potential, IPCC 2021 GWP20 V1.03 and IPCC 2021 GWP100 V1.03, methodology was used, based on the 2021 Report of the Intergovernmental Panel on Climate Change Guidelines for Global Warming Potential, with 20 and 100-year time horizons, respectively, measured in kg CO_2-eq. This impact category was considered due to the central objective of CO_2 mitigation in fermentation processes.

Water-related impacts (AWARE) were considered particularly relevant due to the water scarcity issue often faced in wine-producing regions. In this regard, the water requirement of auxiliary technologies is a vital factor. For calculating the water footprint, AWARE V1.06 is used, a methodology that is a regionalized, water use midpoint indicator representing the relative Available Water REmaining per area in a watershed after the demand of humans and aquatic ecosystems have been met. The only category is Water Use, measured in m^3.[18]

Regarding the toxicity, USEtox 2 (recommended + interim) V2.14 was used, which focuses on an environmental model for the characterization of human and eco-toxicological impacts. The categories that were assessed were Human Toxicity, Cancer – cases; human toxicity, non-cancer – cases. The inclusion of this impact category is to help to assess the potential burden shifting associated with the technology design. This assessment aimed at ensuring that the reductions in climate change impacts are not achieved at the expense of excessively increased toxicity burdens of the winery.

Goal and scope. For this study, a functional unit of 1 g of CO_2 from wine fermentation, captured by column absorption or electro-absorption, is used. The study compares the environmental performance of the electro-absorption and column absorption based on the same functional unit of 1 g CO_2 captured. For each capture process, the experimentally determined optimal operating conditions were used as foreground data in the LCA modelling. The environmental impacts were normalized per unit of CO_2 captured, ensuring comparability between the two configurations. Fig. 2 illustrates the system boundary of the study. The LCA considered five scenarios of the two capture processes:

- Scenario 1 (Sc. 1): EDEN® electro-absorption using cell B.
- Scenario 2 (Sc. 2): EDEN® electro-absorption using cell C.
- Scenario 3 (Sc. 3): EDEN® column absorption using cell B.
- Scenario 4 (Sc. 4): EDEN® Column absorption using cell C.
- Scenario 5 (Sc. 5): column absorption using commercial NaOH (Benchmark scenario).

The system studied considers a cradle-to-gate approach, taking into account the different components for technology EDEN® assembly, and also the energy, feedstock, and resources that were used for capturing the CO_2 that comes from a real scenario of the wine fermentation process. The uncaptured CO_2 was not considered as an environmental impact of the system; however, the captured CO_2 was modelled as an emission saving to allow the calculation of the net environmental score of the capture technology.

While synthetic brine was used experimentally to ensure reproducibility, the environmental and economic assessments considered a brine solution sourced from a waste stream to reflect realistic waste brine utilization scenarios. This assumption is backed by a previous study, Requena-Leal *et al.*,[19] by our research group, where water from the industrial rejection stream of the vineyard, reverse osmosis, electrodialysis, seawater, and porewater demonstrated promising potential as an

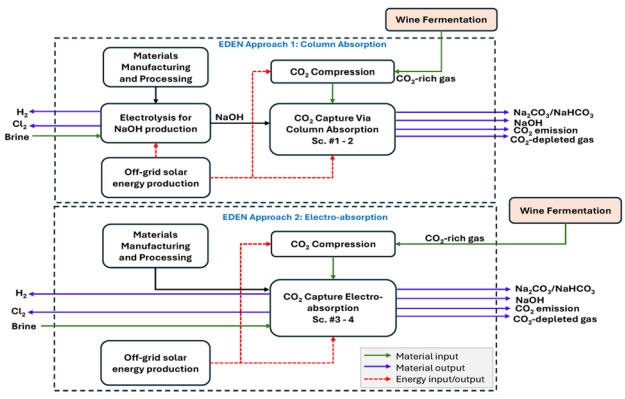

Fig. 2 General scheme of the LCA system boundary definition for the two capture approaches. On the top, column absorption system, and at the bottom, electro-absorption system.

alternative to synthetic brine in chlor-alkali electrolysis. Following this assumption, the brine usage does not add an environmental burden to the system boundary.

The theoretical stoichiometric ratio for the reaction between NaOH and CO_2 is 2 : 1. However, the experimental study showed an average carbon capture efficiency of 80%. Therefore, the LCA modelling assumes an effective molar ratio of NaOH/CO_2 = 2.5 to account for the incomplete capture efficiency. Under these conditions, Na_2CO_3 is considered the final product of the CO_2 capture reaction. The formation of Na_2CO_3 was considered a stable storage pathway within the system boundary, and the captured carbon was assumed not to be re-released to the atmosphere during the assessed life cycle. This assumption represents a scenario in which the produced carbonate is either stored or used in downstream applications without thermal decomposition. The potential long-term release of CO_2 from carbonate conversion processes was therefore not included in the base-case LCA model.

The system also assumed the durability of the two anodic materials was the same under laboratory-scale conditions.

The material balance according to the system boundaries is presented in Fig. 3. Table S1 shows the different materials and quantities considered for each scenario studied.

Economical allocation was considered for the co-products obtained with the multifunctional EDEN® technology (NaOH, Cl_2, and H_2), following guidelines proposed by Guinée *et al.*[20] Since the produced NaOH was used as the absorbent in the capture of the CO_2, its allocated impacts were therefore used in calculating the environmental impact per the functional unit. The allocation proportions calculated using the data from the mass balance and the market prices of the products are presented in Table 2. The study considers the current European market price for the products, and prices obtained in USD were converted to euros.[21]

Material selection. A list of materials was selected from the database, using the closest available equivalents for each one. The configuration for the electrolysis cell includes titanium for both the cathode and the anode, coated with ruthenium and platinum catalysts over carbon black with PTFE. Titanium is also used for cell B as a catalyst in the anode. Nafion serves as the membrane, with silicone for the gaskets, stainless steel for the support screws, and methyl methacrylate for the end and bipolar plates. The storage and connections are made of silicone, and the tanks are made of methyl methacrylate. Additionally, a compressor, two pumps, and the DC power supply are included in the system. For the absorption system columns, polyethylene terephthalate and ethylene glycol are used for the plastic body, with glass spheres of borosilicate, stainless steel for the screws, and silicone for the gaskets. The feedstock consists of sodium chloride for Sc. 1 to Sc. 4, and commercial sodium hydroxide for the benchmark scenario (Sc. 5). Photovoltaic energy is used as the electricity source. The cradle-to-gate inventory data for the EDEN® technology in the carbon capture scenarios, within the assumed system boundaries, are detailed in Table S1.

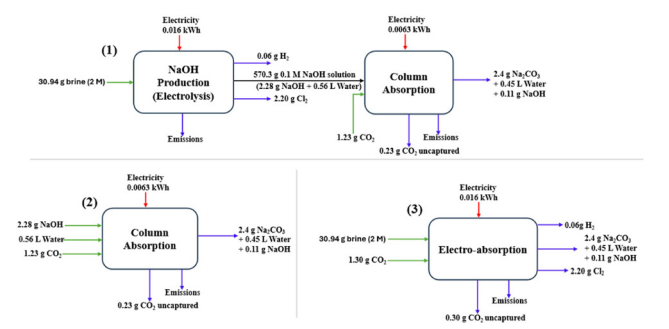

Fig. 3 Material balance of the CO_2 capture scenarios per functional unit.

Table 2 Environmental impact allocation to co-products based on economic value

Products	Amount produced, g per FU	Economic value, EURO per kg	Value, EURO per FU	Proportion
H_2	0.06	6.60	0.00059	0.234
Cl_2	2.20	0.35	0.00077	0.440
NaOH	2.27	0.25	0.00057	0.326

Sensitivity analysis. A sensitivity analysis on energy consumption was conducted to assess the high energy dependence of the system. The modelling considers the electricity mix of major wine-producing countries, including Spain, France, Italy, Chile, and California, as well as other forms of renewable energy, including Spanish grid-based photovoltaic energy, Spanish wind energy, and Spanish nuclear energy. Additionally, a break-even analysis was performed by expressing the net GWP100 as a function of electricity carbon intensity, while treating all other factors as constant. The break-even analysis model can be represented as:

$$Y_{GWP} = k_1 + X \times Z - k_2 \quad (2)$$

where; Y_{GWP} is the net GWP100 (g CO_2-eq. per functional unit), k_1 is the GWP100 from all non-electricity contributions (materials, feedstock, manufacturing, *etc.*), X is the electricity carbon intensity (g CO_2-eq. per kWh), Z is the electricity consumption per functional unit (kWh per FU), and k_2 is the CO_2 captured per functional unit expressed as g CO_2-eq. credit.

At break-even, Y_{GWP} = 0;

$$X = \frac{k_1 - k_2}{Z} \quad (3)$$

The X value was varied parametrically over a range of 0–1000 g CO_2-eq. per kWh in order to evaluate the dependence of the net GWP100 on the emission factor of the electricity supply. This range does not represent specific electricity mixes but was selected to span the full spectrum from fully renewable to highly carbon-intensive electricity systems, thereby enabling identification of the threshold at which the process shifts from net CO_2 reduction to net CO_2 emission. The analysis considered the best-case scenario for each capture

approach and then benchmarked them against scenario 5. This ensures a comprehensive comparison and provides critical insight to guide future implementation.

Life cycle cost. A preliminary LCC analysis was conducted to assess the economic viability of the various carbon capture scenarios. The cost analysis comparison was based on the optimal operating conditions of the two capture processes, normalized on a common scale, EUR (€) per g CO_2 captured. Consistent with the LCA's system boundary, the LCC analysis was based on a cradle-to-gate perspective. The analysis considered the capital cost of the setup components, raw material inputs, energy cost, labour cost, and environmental prices of emissions. Market-average unit prices (€ per unit) for materials, energy cost, and labour cost were sourced from current literature and supplier catalogues. The costs of materials were amortized over their expected lifespan. The environmental prices of emissions were calculated with the SimaPro software using the Environmental Prices (H) V1.00 methodology, developed by CE Delft, and characterized by considering ReCiPe Midpoint 2016 (H) for the environmental burdens.[22]

Due to the smaller values obtained, the prices were normalized to 1 kg of CO_2 captured, to ensure easy readability and understanding. The system boundary also accounted for a potential revenue stream from the commercialization of H_2, Cl_2, and Na_2CO_3, which were modelled as negative costs to reflect their economic offset. The revenue is regarded as potential, since the study does not account for product recovery and purification costs. A sensitivity study of the economic viability of the best scenarios was conducted, considering the electricity source, in major wine-producing countries, consistent with the LCA modelling.

Results

Evaluation of electrolysis performance

In optimizing the electrolysis operating conditions, the effects of the anodic electrode type, cell configuration, and applied voltage were considered. In a chlor-alkali system, the hydrogen evolution reaction (HER) at the cathodic compartment results in the reduction of H^+ to H_2 and the generation of OH^- ions, while the chlorine evolution reaction (CER) at the anodic compartment leads to the oxidation of chloride ions to chlorine gas.[23] The rates of these two reactions are influenced by the current density, which is directly related to the applied voltage and the cell resistance, as well as the electrodes' performance.[23,24] The influence of these factors on the production of H_2, Cl_2, and NaOH was evaluated, and the obtained results are presented in Fig. 4.

Fig. 4A and B present the hydrogen and chlorine volumes obtained under the different experimental conditions. At 6.5 V, both gas volumes were markedly higher than at 5.5 V, reflecting the increase in current density and reaction rate with higher applied voltage. For example, in cell C, the current densities at 6.5 V and 5.5 V were 0.203 A cm^{-2} and 0.148 A cm^{-2},

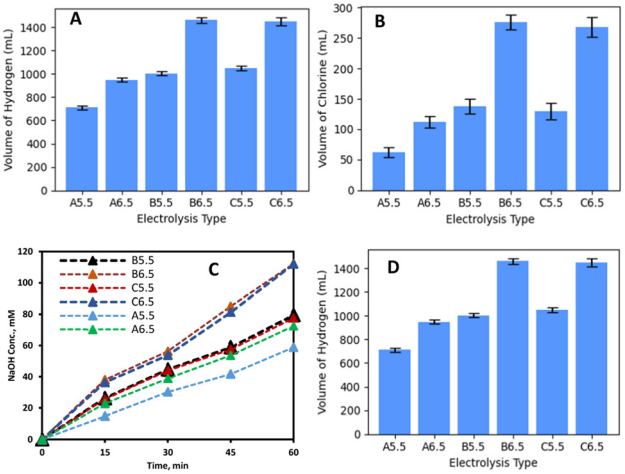

Fig. 4 (A) NaOH production for different scenarios, (B) volume of Cl_2 produced, (C) NaOH concentration through time, (D) specific power (kWh per kg NaOH).

respectively. Across all tested conditions, the faradaic efficiency for hydrogen production remained consistently high (98–100%), confirming that no side reactions occurred at the cathode. In comparison, cell B generates larger volumes of gases than cell A, despite both employing the same cathode and anode materials. This highlights the influence of the electrode gap distance, which is the only difference between the two cells.

Cell A with a larger gap distance experiences higher current resistance than cell B. Hence, at the same voltage, cell B recorded a higher current density than cell A. Comparing cells B and C, they demonstrate similar performance in both hydrogen and chlorine production. The two cells have the same design configuration and electrode gap distance, so with the same cathode material, the similarity in hydrogen production was expected. However, cells B and C have different anodic electrodes; the similarity in chlorine production means the two electrodes exhibit comparable performance under the tested conditions. For all tested conditions, the volume of chlorine gas measured was much lower than that of hydrogen gas, although the stoichiometric coefficient of the overall reaction is a 1 : 1 ratio. This difference could be attributed to the difference in their solubility in water. Chlorine is more soluble in water than hydrogen; hence, some of the chlorine is hydrolysed to form hypochlorous acid (HClO) or hypochlorite ions (ClO^-), thereby reducing the volume of chlorine released.[25,26] The chlorine hydrolysis was confirmed by measuring the ClO^- concentrations in both compartments, of which a significant ClO^- concentration was detected at the anodic compartment, while a negligible amount was detected in the cathodic compartment (Fig. S1 in SI). The negligible ClO^- concentration in the cathodic side also implies that there was no crossover of the chlorine to the cathodic side, indicating the excellent performance of the Nafion® PEM in separating the chlorine and hydrogen, while permitting Na^+ crossover, which is consistent

with a previous study of our group.[17] As shown in Fig. S2, the pH of the anolyte was observed to decrease with time, indicating an acidic media, which also confirm the hydrolysis of chlorine, while the pH of the catholyte increases due to the production of hydroxide ions.

In the cathodic compartment, a linear production rate of sodium hydroxide was observed for all tested conditions, as shown in Fig. 4C. As can be clearly observed, the 6.5 V recorded a higher production rate than the 5.5 V. This observed trend was expected, as faster HER kinetics were observed with the 6.5 V, which means faster hydroxide ion production. For the same applied voltage, cell B outperformed cell A but recorded a similar performance with cell C. Since all the cell types used the same cathode material, the efficiency of sodium hydroxide production is therefore governed by the faradaic efficiency of hydrogen production, membrane transport properties, and operating conditions.

In addition, Fig. 4D shows an overview of the specific power requirement for NaOH production for the studied electrolysis conditions. Although operation at 6.5 V exhibited faster HER and CER kinetics, leading to higher hydrogen and chlorine volumes as well as increased sodium hydroxide concentration, this condition proved to be significantly more energy-intensive. Comparatively, an applied voltage of 6.5 V required more energy per unit of sodium hydroxide produced, approximately 4.36 kWh kg^{-1} NaOH, than 5.5 V, which consumed 3.10 kWh kg^{-1} NaOH in cells B and C, respectively. This increase is commonly attributed to higher overpotentials, enhanced bubble formation, and greater heat losses associated with elevated operating voltages.[27] Due to the additional resistance in cell A, it exhibited comparatively higher specific power requirements at both 5.5 V and 6.5 V than the corresponding values for cells B and C. This indicates that operating at 5.5 V is more energy-efficient for the EDEN® technology. Nevertheless, even under the most favourable conditions, the specific energy demand remains above the values reported for industrial chlor-alkali membrane processes (2.10–2.15 kWh kg^{-1} NaOH).[29] It is important to note that industrial systems typically employ highly concentrated brine solutions (~5 M), whereas the process investigated here relies on low-concentration brine, which can be sourced from industrial waste streams, such as electrodialysis,[30] or from groundwater. At such low concentrations, reduced ionic conductivity, mass transfer limitations, and limited Na^+ availability constrain sodium hydroxide production, thereby increasing the specific power requirements.[28]

Evaluation of the CO_2 capture performance

The CO_2 capture can be tailored towards the formation of sodium carbonate or sodium bicarbonate. Fig. 5A and B depict the time-dependent formation of sodium carbonate and sodium bicarbonate during 105 minutes of CO_2 absorption using the column absorption approach, emphasizing the influence of NaOH concentration on the carbonate species formed. As shown in Fig. 5A, when a low NaOH concentration (0.05 M) was employed, two distinct product formation stages were observed: sodium carbonate (Na_2CO_2) dominated up to approximately 40 minutes, after which the reaction shifted toward the formation of sodium bicarbonate ($NaHCO_3$). In Fig. 5B, when a higher NaOH concentration (0.15 M) was employed, sodium carbonate (Na_2CO_2) formation dominated throughout the 105 minutes of CO_2 absorption, with no sodium bicarbonate ($NaHCO_3$) detected. Under these conditions, either the CO_2 flow rate or the absorption duration becomes the limiting factor. By contrast, in the electro-absorption approach, Na_2CO_2 was the sole product observed across all experimental conditions, as shown in Fig. S3. This indicates that within the applied voltage studied, the NaOH production rate was higher than the NaOH consumption rate, resulting in excess OH^- ions. In a similar study by Mahmoudian *et al.*,[29]

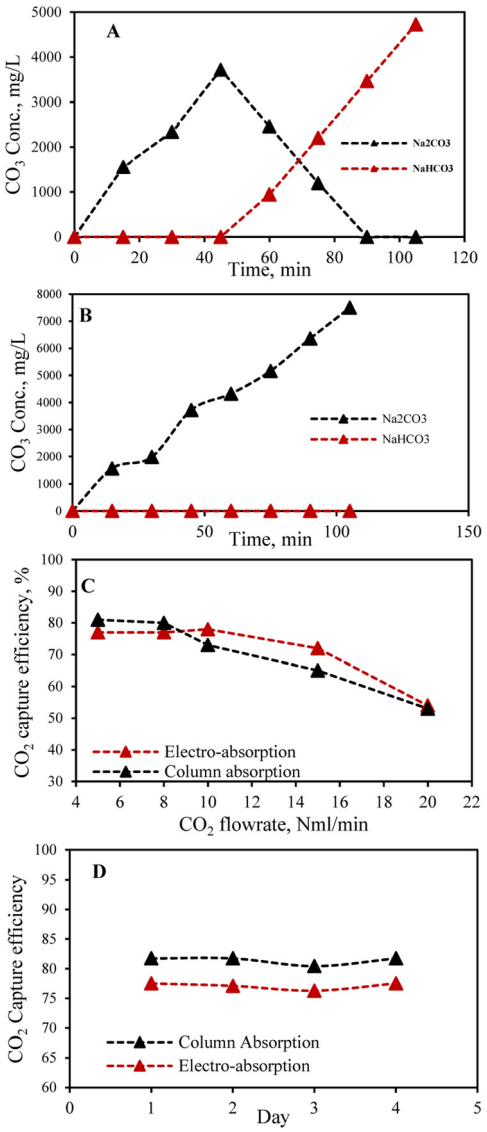

Fig. 5 Carbon capture evolution (A) column absorption with 0.05 M NaOH, (B) column absorption with 0.15 M NaOH, (C) CO_2 capture efficiency (pure) for column absorption and for electro-absorption, (D) CO_2 capture efficiency (from wine fermentation) for column absorption and for electro-absorption.

where a relatively higher CO_2 flow rate was used for the electro-absorption process, the OH^- ions were the limiting factor, and the study reported the formation of $NaHCO_3$ without Na_2CO_3.

This work aimed to evaluate CO_2 capture using the electrochemical EDEN® technology through two different approaches: (i) a conventional absorption column and (ii) the electrochemical cell itself acting as an absorber (electro-absorption). Both approaches were tested with CO_2 supplied from a pressure canister (pure CO_2) as well as from a fermenter, in order to assess the applicability of the proposed technology in a real industrial scenario such as the winery sector. Fig. 5C illustrates the influence of CO_2 flow rate on capture efficiency for both column absorption and electro-absorption using pure CO_2. Capture efficiency decreased as the CO_2 flow rate increased, with optimal values observed at 8 Nml min^{-1} for the column and 10 Nml min^{-1} for electro-absorption. This inverse relationship arises from reduced gas–liquid interaction time at higher flow rates.[33] Owing to the relatively small dimensions of the electrolyzer and column, faster CO_2 feed rates limit residence time, thereby constraining mass transfer and chemical interaction between CO_2 and NaOH molecules, which lowers capture efficiency. Conversely, lower flow rates enable prolonged interaction, resulting in improved absorption performance. For column absorption, however, variations in NaOH flow rate showed no statistically significant effect on capture efficiency under the studied conditions, shown in Fig. S4A. As presented in Fig. S4B, the capture efficiency increases with increasing the starting concentration of NaOH solution. Within the tested CO_2 flow rate and experimental duration, the capture efficiency remains constant for NaOH concentrations of 0.1 M and above. This could be attributed to a sufficient amount of the OH^- ions within the tested range.

When the optimized operating conditions for both column absorption and electro-absorption were applied to capture CO_2 emitted directly from wine fermentation, the results demonstrated the technology's potential to function effectively under real-world conditions. As shown in Fig. 5D, both approaches maintained consistent daily capture efficiencies throughout the fermentation period. The column absorption system achieved slightly higher efficiency than electro-absorption, consistent with the trends observed using pure CO_2. Moreover, for each approach, the capture efficiency with fermentation-derived CO_2 did not differ significantly from that obtained with pure CO_2, with deviations below 2%.

The daily progress of the wine fermentation and the corresponding analysis of the produced wine are provided in Fig. S5 and Table S3, respectively.

Global warming potential in CO_2 capture scenarios

The global warming potential (GWP) and the components' contributions to the GWP for the different scenarios studies over periods of 20 and 100 years are represented in Fig. 6A and B, respectively. The carbon balance is based on the CO_2-eq. of all GHGs emitted relative to the amount of CO_2 captured. As can be observed in Fig. 6A, under the studied conditions and assumptions, all the studied scenarios recorded carbon

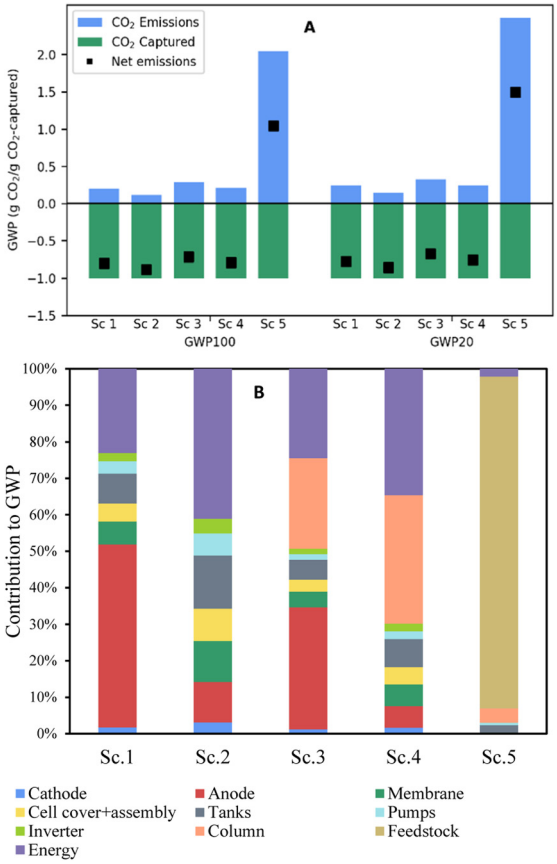

Fig. 6 (A) Carbon footprint (GWP100 and GWP20) of the different scenarios evaluated, (B) contribution of materials + energy to GWP100 for the different scenarios.

savings except for scenario 5, conventional column absorption using commercial NaOH. The net carbon footprint of scenario 5 is positive, indicating this capture scenario will result in an increase in the winery's carbon footprint instead of its reduction. The main contributor to the GWP of this scenario is the feedstock (commercial NaOH), which can be explained by the dependence on fossil-based grid mixes for most commercial NaOH production.[30,31] The electrochemically produced NaOH for scenarios 1 to 4 relies on renewable energy; as a result, the four scenarios recorded a negative carbon footprint for both long-term and short-term periods, demonstrating their ability to reduce the carbon footprint of the winery. Among these four scenarios, a performance comparison can be made between the electrolyzer cell types and the two capture approaches studied.

In terms of the cell types, cell C recorded a relatively lower impact than cell B in both electro and column absorption, with the difference driven mainly by the environmental impact of their anode material. For instance, in the electro-absorption, the anode in cell B (Sc. 1) accounts for over 60% of the total impact, while that of cell B (Sc. 2) accounts for <20% of the total impact. This observation highlights the importance of material optimization in the design of the electrochemical

system. Given that both cells exhibited similar performance in the electrolysis process, the anode used in cell C can be considered more environmentally friendly than cell B. However, it is important to mention that the durability (lifespan) of the two anodes was considered the same within the context of a laboratory-scale process, an assumption that may not hold for industrial operation. This is because cell B anode is made with a titanium plate, while cell C anode is made with titanium felt, and the former is known to be more durable in industrial processes than the latter.[32]

Between the two capture approaches, with the same type of cell, the electro-absorption recorded the lower carbon footprint, which can be attributed to its simplified design and hence involved a lesser number of material components compared to the column absorption approach. However, since the CO_2 capture efficiency of the electro-absorption is not 100%, the column absorption approach presents the chance to produce a higher pure H_2 than the former. As a result, if the system boundary is expanded to include the purification of the co-products and their avoided emissions, the carbon footprint difference between these approaches will be reduced significantly. Another factor with a significant contribution to the GWP of the studied scenarios is the energy requirement of the capture processes. The contribution to the GWP is more prominent in scenarios 2 and 4, contributing about 30% of the total impact. Generally, electricity usage is responsible for a greater share of the carbon footprint of electrochemical systems, because of the heavy share of fossil fuels in many regional electricity mixes.[33–35] The relatively lower fraction recorded under these scenarios is primarily due to the system's reliance on 100% renewable energy, off-grid solar energy, and is hence susceptible to change with a change in energy source.

The GWP for the long-term (100 years) recorded slightly lower impact than the short-term (20 years), but the ranking of the scenarios did not change. This decrease in impact is because, within a short period, greater emphasis is placed on short-lived but highly potent greenhouse gases such as methane and nitrous oxide. Thus, the 20-year GWP metric captures immediate climate forcing and near-term warming impact, while the 100-year GWP spreads the impact over a longer period, contributing to short-lived gases appearing less significant.[36,37] Overall, scenarios 1 to 4 recorded a net negative GWP for both short and long term, irrespective of the type of cell or the capture approach employed. Comparatively, scenarios 1, 2, 3, and 4 recorded net GWP of −0.804, −0.882, −0.717, and −0.794 g CO_2-eq. per g CO_2 captured, respectively, indicating that scenario 2 can be considered the most environmentally suitable implementation route under the studied system boundary and assumptions.

While the formation of Na_2CO_3 was considered a stable carbon storage pathway within the defined system boundaries, its long-term permanence depends on its subsequent use. Sodium carbonate is a key intermediate in soda–lime glass production, widely used in wine bottle manufacturing,[38] which could enable integration within the wine value chain and support circular economy strategies through reuse and recycling of packaging materials. Alternatively, Na_2CO_3 may be applied to agricultural soils, where inorganic carbon can remain stored over long periods under suitable conditions.[39] However, the stability of carbonate-based storage depends on the end-use pathway, as some industrial processes, such as glass production, may involve thermal decomposition that releases CO_2.[40] Therefore, future studies should evaluate the full life cycle of carbonate utilization to better quantify its long-term carbon permanence.

The results herein can be compared with other LCA studies of decarbonization processes with a functional unit of CO_2 captured and a cradle-to-gate system boundary. In this context, Medina-Martos *et al.*[41] studied the environmental footprint of using NaOH as an absorbent for CO_2 capture to produce carbonates, within a cradle-to-gate system boundary. The study employed a scenario-based assessment and reported a carbon footprint of −0.32 and 0.54 kg CO_2-eq. per kg CO_2 captured for renewable energy-based NaOH and commercial NaOH, respectively. Outside the field of NaOH-based carbon capture, Leonzio *et al.*[42] conducted an LCA on direct air capture using sorbents within a cradle-to-gate system boundary. They reported an overall emissions of −116 kg CO_2-eq. per ton CO_2 captured (equivalent to −0.116 g CO_2-eq. per g CO_2 captured) for a cellulose-based amine sorbent capture system. Similarly, Deutz *et al.*[43] evaluated the carbon reduction potential of a direct air capture system based on temperature-vacuum swing adsorption employing a cradle-to-gate system boundary and reported a net emission of −0.854 kg CO_2-eq. per kg CO_2 captured. Consistent with the findings presented herein, all these studies reported that the capture systems performed better with renewable energy sources. The results herein can therefore be said to be in the range of values reported in literature, and indicate a great potential of the EDEN® technology in carbon footprint reduction. However, it is important to state that these comparisons were not made in a definitive benchmark context because of variations in data sources, assumptions, and software/database versions, which typically have a significant influence on LCA results. The comparison only seeks to contextualize the technology's environmental performance relative to existing technologies.

Water footprint in CO_2 capture scenarios

Given that many wine-producing regions face seasonal water scarcity, it is necessary to quantify the water footprint of auxiliary technologies to be integrated into the winery to ensure their long-term sustainability and resilience. On this basis, the AWARE methodology was used to quantify the total water use of the different carbon capture scenarios, and the results are presented in Fig. 7. Consistent with many decarbonization technologies, all the studied scenarios recorded a net-positive water footprint, an observation that is due to the primary purpose of decarbonization technologies, designed to reduce CO_2 emissions and not water consumption.[44,45] These results suggest that the integration of the CO_2 capture unit into the industry will increase the industry's water footprint. Among

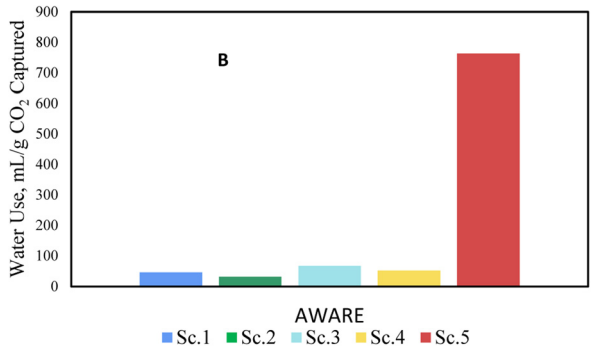

Fig. 7 Water footprint of the different CO_2 capture scenarios.

the capture scenarios, scenario 2 recorded the lowest water use of 32.0 mL g^{-1} CO_2 captured, while scenario 5 recorded the highest water footprint, driven mainly by upstream processes. The higher water use for scenario 5 can be explained by the fact that commercial NaOH production demands fresh water for brine preparation, cooling, and shares a fraction of the water footprint of the grid mix.[46,47] Additionally, the preparation of the NaOH solvent for the column absorption requires a significant volume of freshwater, which contributes to the overall relatively higher water footprint.

The lower water footprint recorded for scenarios #1–4 is mainly due to the circular economy principle employed, by turning industrial waste brine into a feedstock for CO_2 capture. This strategy reduces the technology's demand for freshwater, thereby providing environmental credit.

Toxicity impact in CO_2 capture scenarios

For different scenarios, human health toxicity in cancer and non-cancer cases was calculated using the UseTox Methodology, which also includes the freshwater ecotoxicity factor, represented in Fig. 8.

From the studied scenarios, Sc. 5 reaches the highest toxicity for human health, above 6E-7 Cases of cancer/non-cancer per g of CO_2 captured, exhibiting the importance of the materials and feedstock mainly due to the direct use of commercial NaOH. On the other hand, the EDEN® technology scenarios recorded less impact than the commercial options. Cancer cases are less than the non-cancer cases for EDEN® scenarios.

The lowest impact on human health corresponds to Sc. 2 (cell C), which uses the in-house synthesized anode. This is mainly because it is approximately 6 times lighter than the commercial option in cell B, used for Sc. 1 and Sc. 3, although both use similar materials, such as titanium, ruthenium, and platinum.

Regarding freshwater ecotoxicity, a similar trend is observed, with Sc. 5 having a greater impact than the EDEN® technologies. Using cell C yields the lowest ecotoxicity values, approximately 7400 PAF m^3 day per g CO_2 captured, regardless of the method used for carbon absorption, although electro-absorption is slightly less toxic than column absorption.

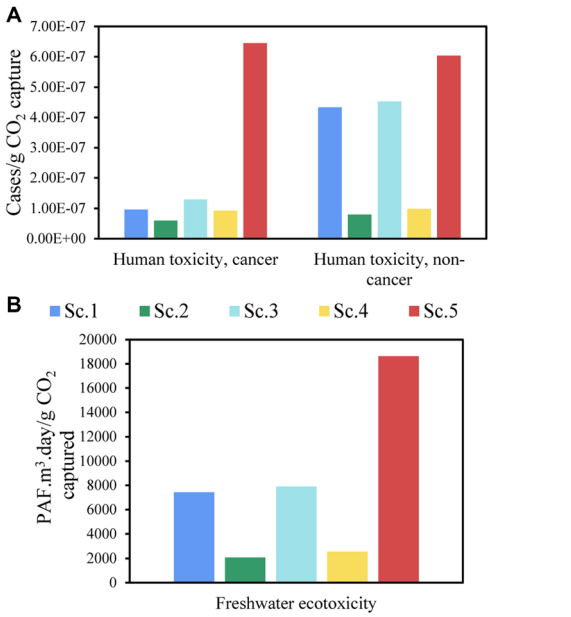

Fig. 8 (A) Human toxicity in cancer and non-cancer cases for the different scenarios, (B) freshwater ecotoxicity for different scenarios.

Column absorption with cell B exhibits the highest impact on freshwater ecotoxicity among the EDEN® alternatives.

Sensitivity analysis

Given that the electricity consumption has a significant influence on the GWP of the carbon capture scenarios, their overall environmental performance depends on the energy source/type. The sensitivity analysis provides insight into how regional and technological variations in electricity production influence the carbon footprint of the studied CO_2 capture scenarios. Fig. 9 presents the influence of different electricity sources on the GWP100 impact of the two capture approaches using the best-performing scenarios (shown in Fig. 6), 2 and 4, benchmarked against scenario 5. The analysis is conducted across the electricity mix of the leading wine-producing countries and various renewable energy types in Spain.

The results shown in Fig. 9 indicate that the GWPs of the carbon capture scenarios are highly sensitive to energy sources, recording significant variability across national electricity mixes and renewable energy types. The variability in GWP observed is directly related to the carbon intensity of the different electricity sources.[48]

For the five national electricity mixes, the GWP is at least 43% higher compared to the base energy (off-grid photovoltaic). The variability is less when comparing the GWP of the different renewable energy sources to the GWP of the base energy, with grid-based photovoltaic and wind energy recording at least 1.3% higher, while nuclear energy recorded 3% lower than the base energy. Among the capture scenarios, scenario 2 maintained the lowest GWP across all the energy sources/types, followed by scenario 4. The two scenarios recorded a net negative GWP across the renewable energy

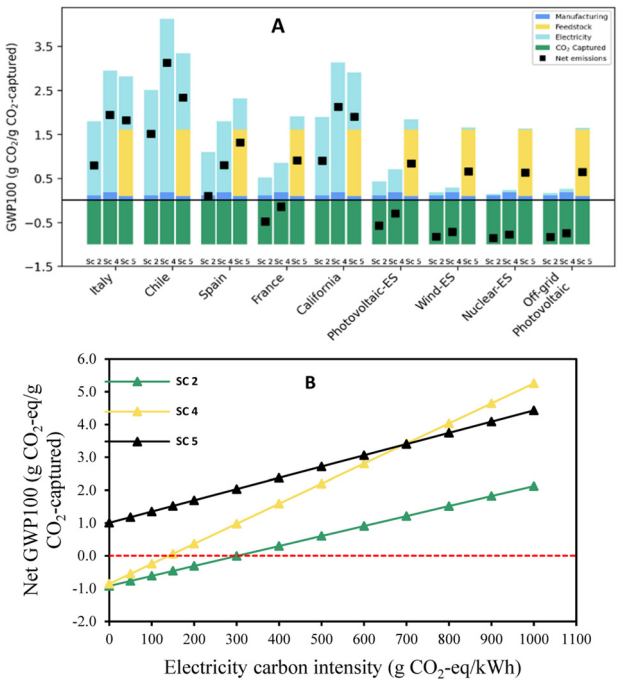

Fig. 9 Sensitivity of net GWP100 to electricity source and carbon intensity: (A) results for different electricity mixes and renewable energy scenarios, (B) break-even analysis as a function of electricity carbon intensity.

types. However, across the national electricity mix, all scenarios recorded net positive GWP, except for France's electricity mix, where both scenarios 2 and 4 recorded net negative GWP. This clearly indicates that the carbon capture scenarios performed better under renewable energy than the national electricity mix. Across energy sources, the electricity component is the major contributor to the GWP of scenarios 2 and 4, except for wind, nuclear, and off-grid photovoltaic energy, where manufacturing is the major contributor.

Given the significant contribution of electricity usage to the net carbon footprint, a break-even analysis was performed by expressing net GWP100 as a function of electricity carbon intensity, while the combined influence of all other factors was modelled as a constant. The results, as shown in Fig. 9B, further confirm the strong influence that the type/source of electricity has on the environmental performance of the system. A clear break-even point can be observed for scenarios 2 and 4, below which the process yields a net reduction in CO_2 emissions and above which the environmental benefits are lost. These threshold values indicate that scenario 2 maintains a net-negative climate impact as long as the electricity carbon intensity remains below approximately 300 g CO_2-eq. per kWh, which corresponds to moderately decarbonized electricity grids, such as those represented by current European electricity mixes (*e.g.*, France and Spain, according to the Ecoinvent database). In contrast, scenario 4 is environmentally favourable only when the electricity's carbon intensity is below approximately 150 g CO_2-eq. per kWh, which requires low-carbon electricity sources, such as those dominated by renewable or nuclear energy. Scenario 5 does not achieve a net emissions reduction within the analyzed range, mainly because its major carbon emissions contribution comes from the feedstock. These results highlight that the carbon reduction potential of the EDEN® systems strongly depends on the use of low-carbon electricity sources.

Trade-off between carbon capture efficiency and GWP for the capture approaches

In determining the most sustainable operation conditions of the capture scenarios, a trade-off between CO_2 capture efficiency and global warming potential was observed. As illustrated in Fig. 10A, the grams of CO_2-eq. emissions per gram of CO_2 captured decrease with increasing CO_2 inflow rate, while the CO_2 capture efficiency also decreases over the same range. This phenomenon presents enhanced environmental sustainability of the system at the expense of lower capture efficiency or *vice versa*. For the two scenarios, the trade-off manifested strongly in scenario 2, in terms of magnitude and sensitivity. This phenomenon is because, in the electro-absorption approach, a more favourable ratio of CO_2 captured to energy input is attained at higher flow rates, which in effect reduces the life cycle emissions per unit CO_2 captured. The same phenomenon applies to the column absorption approach; however, over 90% of its energy consumption is attributable to electrolysis for NaOH production, which is independent of the CO_2 inflow rate. As a result, energy savings with increasing flow rate are insufficient to cause a significant change in GWP100, making the column's overall GWP100 less sensitive to flow rate. In contrast, its CO_2 capture efficiency is sensitive to the CO_2 flow rate.

In terms of the trade-off between carbon footprint and capture cost, a linear relationship was observed, as shown in

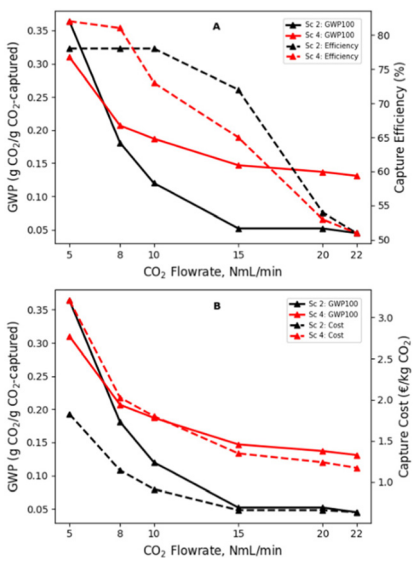

Fig. 10 Trade-off between (A) the capture efficiency and GWP100, and (B) the capture cost and GWP100 for the best scenarios.

Fig. 10B. This observed trend indicates that both environmental and economic impacts are primarily governed by the amount of CO_2 captured at different flow rates. Since the main operational and infrastructure burdens remain constant, increasing the CO_2 flow rate results in a faster capture rate, which reduces both the environmental impact and the cost per unit of captured CO_2. Therefore, no strong trade-off between environmental and economic performance was observed within the studied range of operating conditions. However, the combined trade-off among carbon footprint, capture cost, and capture efficiency suggests that the flow rate is an important factor to consider for future optimization or implementation by finding a balance between minimizing life cycle emissions, capture cost, and maintaining sufficiently high capture efficiency. Revisiting the previous assertion, the optimal flow rate for the column absorption approach is truly 8 Nml min^{-1}; at this flow rate, the system achieved an 81% capture efficiency at relatively reduced GWP100. However, the 10 ml min^{-1} proposed earlier as the optimal flow rate for the electro-absorption is a bit flexible; depending on whether priority is given to lower GWP100 or higher capture efficiency, the best condition could be either 10 or 15 Nml min^{-1}.

Life cycle costing analysis

As established earlier, the technology sustainability performance is highly sensitive to changes in the type and source of energy, with better performance with renewable energy. The economic viability of scenarios 2 and 4 was assessed across different countries and benchmarked with scenario 5, and the results are presented in Fig. 11. Across the energy sources studied, the national electricity mixes recorded higher capture cost, with the variability mainly driven by the emissions cost. For Italy, Spain, and France, which have relatively higher shares of renewable energy, the major cost component is the energy cost for scenarios 2 and 4. The emission cost is the major cost component for scenario 5, across all the energy sources, due to the higher emissions that are often associated with commercial NaOH production. Aside from the emission cost, a slight variation in energy and labour costs was also observed across the different countries. Chile recorded the lowest energy and labour cost; however, its carbon-intensive electricity nature resulted in higher emissions cost and overall higher capture cost. However, these findings suggest that, if the capture processes are operated with renewable energy in Chile, the net capture cost will be significantly lower than in the other countries under study.

Across all energy sources, the scenarios recorded relatively lower capture costs under renewable energy, with scenario 2 exhibiting the lowest capture cost for all cost components. Comparing scenarios 2 and 4, the difference in material cost is basically due to the cost of procuring an additional unit, the absorption column in scenario 4. In terms of energy cost, the difference can be explained by the longer operation time of Sc. 4, due to the separate electrolysis and column absorption, resulting in extra costs in labour and energy: Sc. 2 operates for 1.08 hours while Sc. 4 operates for 2.3 hours. Overall, the variability in emissions, energy costs, and labour costs across the different regions studied resulted in variations in the net capture costs of capture scenarios.

The lowest capture cost, 0.84 € per kg CO_2 captured, recorded for scenario 2 under the base energy source, is relatively higher compared to the capture cost of the amine-based capture process and the EU average carbon price, at 0.055 and 0.072 € per kg CO_2, respectively.[41,49] However, it is worth noting that the studied processes (Sc. 2 and 4) are at a lower technology readiness level (TRL4). As an emerging solution, the processes are still undergoing optimization and scale-up demonstration, which typically exhibit higher unit costs due to limited economies of scale, experimental component configurations, and less mature supply chains. Generally, low-TRL technologies record high costs during early development phases and achieve cost reduction through optimization, process integration, and industrial scaling.[50–52]

It is worth noting that while the expansion of the system boundary to include the commercialization of the co-products (H_2, Cl_2, and Na_2CO_3) provided potential income, this income could be limited by factors like market volatility and logistical constraints. Under the assumed average market prices, scenarios 2 and 4 yield €1.06, while scenario 5 yielded €0.96 per kg of CO_2, offsetting the capture cost, resulting in a significantly lower net cost, of which scenario 2 recorded a net negative capture cost under the base energy source. However, the volatility of the market price of these products could present a significant uncertainty in the balance. Additionally, the realization of these values in distributed, small-scale applications may be subject to practical constraints. Hydrogen valorization may depend on the availability of local storage, compression, or utilization infrastructure, particularly in decentralized systems such as wineries. Similarly, chlorine commercialization at small production scales may face logistical and regulatory challenges related to storage, transportation, and safety requirements. Consequently, the assumed co-product revenues should be interpreted as theoretical maximum values, and the economic feasibility of implementation may depend on site-specific infrastructure and regulatory conditions.

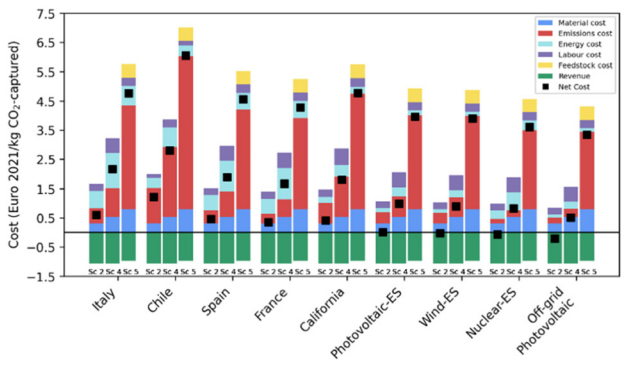

Fig. 11 Sensitivity analysis of the CO_2 capture cost to regional energy source and cost, material cost, and labour costs for selected scenarios.

Conclusions

This study comprehensively evaluates the integration of an electrochemical-based CO_2 capture unit into a winery and assesses the environmental performance through scenario-based LCA modeling. The study demonstrated that the EDEN technology, which is based on the chlor-alkali electrochemical process, can capture CO_2 emissions from industrial processes in a sustainable and cost-effective way, offering a promising technique for climate change mitigation. The experimental results also highlighted the designed system's (EDEN® technology) multifunctionality, converting low-concentration waste brine into hydrogen and chlorine while simultaneously fixing CO_2 in the form of sodium carbonate or sodium bicarbonate.

Regarding the CO_2 capture potential, the technology recorded high capture efficiency within the studied conditions. Additionally, the efficiency of the technology in capturing CO_2 directly from wine fermentation was comparable to its efficiency in absorbing pure CO_2, which highlights the applicability of the technology in real-world carbon capture processes.

The environmental assessment and economic analysis modelled four scenarios of the EDEN® technology and benchmarked them against a fifth scenario (column absorption with commercial NaOH). A net carbon saving at low or even negative capture costs was demonstrated for the EDEN-based scenarios under the study's assumptions. Scenario 2 demonstrated to be the most suitable implementation route, recording the lowest impacts across all categories. The carbon reduction potential of the technology was found to depend on its integration with renewable energy and the possibility of efficiently recovering and commercializing the produced hydrogen, chlorine, and sodium carbonate. The capture cost was highly influenced by the emission cost, which is directly related to the carbon intensity of the electricity source. The commercialization of the products (H_2, Cl_2, and Na_2CO_3) presents an opportunity to reduce the capture cost to net zero or negative capture cost.

These results provide valuable insights into the sustainability performance of the proposed electrochemical CO_2 capture system and its potential for industrial decarbonization. Future work should therefore move beyond laboratory-scale proof-of-concept toward targeted optimization and validation: reduce specific energy consumption through cell and process design improvements, and screen/develop more durable, lower-impact electrode and catalyst materials to minimize lifecycle burdens.

The findings of this work underline the significant climate mitigation potential of integrating electrochemical CO_2 capture within industrial processes such as winemaking. By combining CO_2 capture with the co-production of valuable chemicals and hydrogen, EDEN® demonstrates a pathway toward environmentally and economically viable decarbonization. Furthermore, the technology's capacity to efficiently capture both pure and fermentation-derived CO_2 suggests that its application could extend beyond the wine sector to other industries facing similar biogenic or process-related emissions. This positions EDEN® as a scalable and versatile solution in the broader transition toward low-carbon industrial systems.

Conflicts of interest

There are no conflicts of interests to declare.

Data availability

The data supporting the findings of this study were generated using the SimaPro 10.1.0.6 software. The data supporting this article have been included as part of the supplementary information (SI). Supplementary information: Tables S1 and S2. See DOI: https://doi.org/10.1039/d6gc00309e.

Any additional raw data or background calculations that support the findings of this study are available from the corresponding author upon reasonable request.

Acknowledgements

The authors thank Junta de Comunidades de Castilla-La Mancha and the EU (FEDER) for the financial support through the project SPBLY/21/180501/000075.

References

1 L. H. U. W. Abeydeera, J. W. Mesthrige and T. I. Samarasinghalage, Global Research on Carbon Emissions: A Scientometric Review, *Sustainability*, 2019, **11**, 3972, DOI: 10.3390/SU11143972.
2 M. Filonchyk, M. P. Peterson, H. Yan, A. Gusev, L. Zhang, Y. He and S. Yang, Greenhouse gas emissions and reduction strategies for the world's largest greenhouse gas emitters, *Sci. Total Environ.*, 2024, **944**, 173895, DOI: 10.1016/J.SCITOTENV.2024.173895.
3 Energy Agency, I., World Energy Outlook 2024, 2024.
4 P. Roy, A. K. Mohanty and M. Misra, Prospects of carbon capture, utilization and storage for mitigating climate change, *Environ. Sci.: Adv.*, 2023, **2**, 409–423, DOI: 10.1039/D2VA00236A.
5 B. K. Sovacool, D. F. Del Rio, K. Herman, M. Iskandarova, J. M. Uratani and S. Griffiths, Reconfiguring European industry for net-zero: a qualitative review of hydrogen and carbon capture utilization and storage benefits and implementation challenges, *Energy Environ. Sci.*, 2024, **17**, 3523–3569, DOI: 10.1039/D3EE03270A.
6 R. M. Cuéllar-Franca and A. Azapagic, Carbon capture, storage and utilisation technologies: A critical analysis and comparison of their life cycle environmental impacts, *J. CO2 Util.*, 2015, **9**, 82–102, DOI: 10.1016/J.JCOU.2014.12.001.
7 A. M. Zito, L. E. Clarke, J. M. Barlow, D. Bím, Z. Zhang, K. M. Ripley, C. J. Li, A. Kummeth, M. E. Leonard,

A. N. Alexandrova, F. R. Brushett and J. Y. Yang, Electrochemical Carbon Dioxide Capture and Concentration, *Chem. Rev.*, 2023, **123**, 8069–8098, DOI: 10.1021/ACS.CHEMREV.2C00681.

8 J. L. Galvez-Martos, J. Morrison, G. Jauffret, E. Elsarrag, Y. AlHorr, M. S. Imbabi and F. P. Glasser, Environmental assessment of aqueous alkaline absorption of carbon dioxide and its use to produce a construction material, *Resour., Conserv. Recycl.*, 2016, **107**, 129–141, DOI: 10.1016/J.RESCONREC.2015.12.008.

9 I. Shabir, K. K. Dash, A. H. Dar, V. K. Pandey, U. Fayaz, S. Srivastava and R. Nisha, Carbon footprints evaluation for sustainable food processing system development: A comprehensive review, *Future Foods*, 2023, **7**, 100215, DOI: 10.1016/J.FUFO.2023.100215.

10 State of the World Vine and Wine Sector in 2024.

11 C. Gazulla, M. Raugei and P. Fullana-I-Palmer, Taking a life cycle look at crianza wine production in Spain: Where are the bottlenecks?, *Int. J. Life Cycle Assess.*, 2010, **15**, 330–337, DOI: 10.1007/S11367-010-0173-6/FIGURES/4.

12 Wine industry called out on carbon dioxide emissions – The Real Review, https://www.therealreview.com/2023/05/16/wine-industry-called-out-on-carbon-dioxide-emissions/.

13 C. Pattara, A. Raggi and A. Cichelli, Life cycle assessment and carbon footprint in the wine supply-chain, *Environ. Manage.*, 2012, **49**, 1247–1258, DOI: 10.1007/s00267-012-9844-3.

14 F. F. Montalvo, J. L. García-Alcaraz, E. M. Cámara, E. Jiménez-Macías and J. Blanco-Fernández, Environmental impact of wine fermentation in steel and concrete tanks, *J. Cleaner Prod.*, 2021, **278**, 123602, DOI: 10.1016/j.jclepro.2020.123602.

15 OIV: Global Wine Production Plummets in 2024 – Wine-Intelligence, https://wine-intelligence.com/blogs/wine-analytics-pricing-report-data/oiv-global-wine-production-plummets-in-2024-vinovistara-wine-intelligence?srsltid=AfmBOoobp8oG1Bp7_s8uWtP81k0LPLHGn3ArhVaIHyTzTRBqIaSxTeV_.

16 T. Terlouw, C. Bauer, L. Rosa and M. Mazzotti, Life cycle assessment of carbon dioxide removal technologies: a critical review, *Energy Environ. Sci.*, 2021, **14**, 1701–1721, DOI: 10.1039/D0EE03757E.

17 M. M. Gomaa, I. Requena, R. Granados-Fernández, M. A. Rodrigo and J. Lobato, Optimizing flow configurations and membrane durability in chlor-alkali reversible electrochemical cells, *J. Energy Storage*, 2025, **126**, 116949, DOI: 10.1016/J.EST.2025.116949.

18 SimaPro database manual Methods library, 2024.

19 I. Requena-Leal, C. M. Fernández-Marchante, J. Lobato and M. A. Rodrigo, Towards a more sustainable hydrogen energy production: Evaluating the use of different sources of water for chloralkaline electrolyzers, *Renewable Energy*, 2024, **233**, 121137, DOI: 10.1016/J.RENENE.2024.121137.

20 J. B. Guinée, R. Heijungs and G. Huppes, Economic allocation: Examples and derived decision tree, *Int. J. Life Cycle Assess.*, 2004, **9**, 23–33, DOI: 10.1007/BF02978533.

21 Soda Ash price index – businessanalytiq, https://businessanalytiq.com/procurementanalytics/index/soda-ash-price-index/.

22 C. Delft, *Handboek Milieuprijzen*, 2023.

23 K. Li, Q. Fan, H. Chuai, H. Liu, S. Zhang and X. Ma, Revisiting Chlor-Alkali Electrolyzers: from Materials to Devices, *Trans. Tianjin Univ.*, 2021, **27**, 202–216, DOI: 10.1007/S12209-021-00285-9.

24 J. G. Vos, Z. Liu, F. D. Speck, N. Perini, W. Fu, S. Cherevko and M. T. M. Koper, Selectivity Trends Between Oxygen Evolution and Chlorine Evolution on Iridium-Based Double Perovskites in Acidic Media, *ACS Catal.*, 2019, **9**, 8561–8574, DOI: 10.1021/ACSCATAL.9B01159.

25 G. L. Squadrito, E. M. Postlethwait and S. Matalon, Elucidating mechanisms of chlorine toxicity: reaction kinetics, thermodynamics, and physiological implications, *Am. J. Physiol.: Lung Cell. Mol. Physiol.*, 2010, **299**, L289, DOI: 10.1152/AJPLUNG.00077.2010.

26 M. Alkan, M. Oktay, M. M. Kocakerim and M. Çopur, Solubility of chlorine in aqueous hydrochloric acid solutions, *J. Hazard. Mater.*, 2005, **119**, 13–18, DOI: 10.1016/J.JHAZMAT.2004.11.001.

27 X. Duan, J. Xiao, W. Lin, S. Wang and J. Wen, Experimental and numerical investigation of the impact of operating conditions on water electrolysis with ultrasonic, *Int. J. Hydrogen Energy*, 2024, **49**, 404–416, DOI: 10.1016/J.IJHYDENE.2023.08.066.

28 J. Kamcev, R. Sujanani, E. S. Jang, N. Yan, N. Moe, D. R. Paul and B. D. Freeman, Salt concentration dependence of ionic conductivity in ion exchange membranes, *J. Membr. Sci.*, 2018, **547**, 123–133, DOI: 10.1016/J.MEMSCI.2017.10.024.

29 F. Mahmoudian, I. Requena-Leal, J. Lobato, F. Nabizadeh-Chianeh and M. A. Rodrigo, Integrated electrochemically assisted absorbers for the removal of Carbon dioxide, *Electrochim. Acta*, 2025, **513**, 145556, DOI: 10.1016/J.ELECTACTA.2024.145556.

30 A. Baral, J. L. Galvez-Martos and T. Hanein, Realizing CO2 emission reduction in lime and soda ash manufacturing through anion exchange, *Green Chem.*, 2025, **27**, 3431–3442, DOI: 10.1039/D4GC05568C.

31 L. Rincón, C. Ruiz, R. R. Contreras and J. Almarza, Study of the NaOH(s)–CO_2(g) reaction creating value for industry: green natrite production, energy, and its potential in different sustainable scenarios, *Environ. Sci.: Adv.*, 2023, **2**, 957–966, DOI: 10.1039/D2VA00281G.

32 A Comprehensive Comparison: Titanium Fiber Felt VS. Porous Titanium Plate, *Knowledge*, https://www.toptitech.com/info/a-comprehensive-comparison-titanium-fiber-fel-88475364.html.

33 P. Holzapfel, V. Bach and M. Finkbeiner, Electricity accounting in life cycle assessment: the challenge of double counting, *Int. J. Life Cycle Assess.*, 2023, **28**(7), 771–787, DOI: 10.1007/S11367-023-02158-W.

34 S. Kibria Nabil, S. McCoy and M. G. Kibria, Comparative life cycle assessment of electrochemical upgrading of CO2

to fuels and feedstocks, *Green Chem.*, 2021, **23**, 867–880, DOI: 10.1039/D0GC02831B.

35 L. Rosa, D. L. Sanchez, G. Realmonte, D. Baldocchi and P. D'Odorico, The water footprint of carbon capture and storage technologies, *Renewable Sustainable Energy Rev.*, 2021, **138**, 110511, DOI: 10.1016/J.RSER.2020.110511.

36 D. S. Mallapragada and B. K. Mignone, A theoretical basis for the equivalence between physical and economic climate metrics and implications for the choice of Global Warming Potential time horizon, *Clim. Change*, 2019, **158**(2), 107–124, DOI: 10.1007/S10584-019-02486-7.

37 UNFCCC: UNITED NATIONS Information on Global Warming Potentials, 2004.

38 R. D. Rawlings, J. P. Wu and A. R. Boccaccini, Glass-ceramics: Their production from wastes-A Review, *J. Mater. Sci.*, 2006, **41**, 733–761, DOI: 10.1007/S10853-006-6554-3.

39 R. Lal, Soil Carbon Sequestration Impacts on Global Climate Change and Food Security, *Science*, 2004, **304**, 1623–1627, DOI: 10.1126/SCIENCE.1097396.

40 M. Fernández Bertos, S. J. R. Simons, C. D. Hills and P. J. Carey, A review of accelerated carbonation technology in the treatment of cement-based materials and sequestration of CO2, *J. Hazard. Mater.*, 2004, **112**, 193–205, DOI: 10.1016/J.JHAZMAT.2004.04.019.

41 E. Medina-Martos, J. L. Gálvez-Martos, J. Almarza, C. Lirio, D. Iribarren, A. Valente and J. Dufour, Environmental and economic performance of carbon capture with sodium hydroxide, *J. CO2 Util.*, 2022, **60**, 101991, DOI: 10.1016/J.JCOU.2022.101991.

42 G. Leonzio, O. Mwabonje, P. S. Fennell and N. Shah, Environmental performance of different sorbents used for direct air capture, *Sustainable Prod. Consumption*, 2022, **32**, 101–111, DOI: 10.1016/J.SPC.2022.04.004.

43 S. Deutz and A. Bardow, Life-cycle assessment of an industrial direct air capture process based on temperature–vacuum swing adsorption, *Nat. Energy*, 2021, **6**, 203–213, DOI: 10.1038/S41560-020-00771-9.

44 L. Rosa, D. L. Sanchez, G. Realmonte, D. Baldocchi and P. D'Odorico, The water footprint of carbon capture and storage technologies, *Renewable Sustainable Energy Rev.*, 2021, **138**, 110511, DOI: 10.1016/J.RSER.2020.110511.

45 N. S. Matin and W. P. Flanagan, Life cycle assessment of amine-based versus ammonia-based post combustion CO2 capture in coal-fired power plants, *Int. J. Greenhouse Gas Control*, 2022, **113**, 103535, DOI: 10.1016/J.IJGGC.2021.103535.

46 M. Herrero-Gonzalez and R. Ibañez, Technical and Environmental Feasibilities of the Commercial Production of NaOH from Brine by Means of an Integrated EDBM and Evaporation Process, *Membranes*, 2022, **12**, 885, DOI: 10.3390/MEMBRANES12090885.

47 Good Practices Manual Green House Gases Emission Reduction Chlor-alkali Sector, 2017.

48 I. Munné-Collado, F. M. Aprà, P. Olivella-Rosell and R. Villafáfila-Robles, The Potential Role of Flexibility During Peak Hours on Greenhouse Gas Emissions: A Life Cycle Assessment of Five Targeted National Electricity Grid Mixes, *Energies*, 2019, **12**, 4443, DOI: 10.3390/EN12234443.

49 EU Carbon Permits - Price - Chart - Historical Data - News, https://tradingeconomics.com/commodity/carbon.

50 S. N. Khan, Z. Yang, W. Dong and M. Zhao, Cost and technology readiness level assessment of emerging technologies, new perspectives, and future research directions in H2 production, *Sustainable Energy Fuels*, 2022, **6**, 4357–4374, DOI: 10.1039/D2SE00988A.

51 A. W. Zimmermann, T. Langhorst, S. Moni, J. A. Schaidle, F. Bensebaa and A. Bardow, Life-Cycle and Techno-Economic Assessment of Early-Stage Carbon Capture and Utilization Technologies—A Discussion of Current Challenges and Best Practices, *Front. Clim.*, 2022, **4**, 841907, DOI: 10.3389/FCLIM.2022.841907/BIBTEX.

52 T.-T. Nguyen, V. Martin, A. Malmquist and C. A. S. Silva, A review on technology maturity of small scale energy storage technologies, *Renewable Energy Environ. Sustainability*, 2017, **2**, 36, DOI: 10.1051/REES/2017039.